4-24-2020

Modeling and Experimental Verification of an Unconventional 9-Phase Asymmetric Winding PM Motor Dedicated to Electric Traction Applications

Ersin Yolacan

Mustafa K. Guven

Metin Aydin

Ayman M. EL-Refaie

IEEE Access
Multidisciplinary | Rapid Review | Open Access Journal

Received March 17, 2020, accepted March 29, 2020, date of publication April 6, 2020, date of current version April 24, 2020.

Digital Object Identifier 10.1109/ACCESS.2020.2985669

Modeling and Experimental Verification of an Unconventional 9-Phase Asymmetric Winding PM Motor Dedicated to Electric Traction Applications

ERSIN YOLACAN[1], (Member, IEEE), MUSTAFA K. GUVEN[2], (Senior Member, IEEE), METIN AYDIN[1], (Member, IEEE), AND AYMAN M. EL-REFAIE[3], (Fellow, IEEE)

[1]Mechatronics Engineering Department, Kocaeli University, Kocaeli 41380, Turkey
[2]Tech. Centre, Caterpillar Inc., Peoria, IL 61629, USA
[3]Electrical and Computer Engineering Department, Marquette University, Milwaukee, WI 53233, USA

Corresponding author: Ersin Yolacan (ersin.yolacan@kocaeli.edu.tr)

This work was financially supported by the Kocaeli University BAP Unit under Grant 2016/77 and Grant 2017/086.

ABSTRACT Multi-phase permanent magnet motors are becoming popular in various applications such as high power traction which require low cogging and torque ripple, and reduced noise and vibration. This paper presents the development process of a full order detailed mathematical model for an unconventional nine-phase permanent magnet (PM) motor with asymmetric AC windings. The phase inductances are calculated based on the individual winding functions. Using these parameters, electrical equations for each phase based on the voltages and flux linkages are generated. These equations are transformed into an arbitrary reference frame and the torque equations are developed for the 9-phase motor. A Matlab-Simulink model is then developed for the proposed nine-phase PM motor based on the developed dynamic equations. Finally, the model is validated with the finite element analysis and laboratory testing of the prototype motor. It is shown that the developed mathematical model can be used for such complex asymmetric winding multi-phase PM motors.

INDEX TERMS Electric traction, mathematical modeling, multi-phase machines, nine-phase permanent magnet motors, unbalanced winding motors.

I. INTRODUCTION

Due to recent developments of the semiconductor technologies, high speed microcontrollers, intelligent power electronics modules and introducing the high strength Neodymium-Iron-Boron (NdFeB) magnet materials, wide range of application areas are presented for the permanent magnet (PM) synchronous motors. Because of the various benefits of PM motors such as high power/torque density, high torque-current ratio, high efficiency and quite operation, the use of such motors increases as opposed to other types of brushed or brushless motors especially in transportation and traction applications [1]–[5]. On the other hand, multi-phase PM motors have been gaining popularity in recent years particularly in high power electric and hybrid vehicles as well as defense applications due to the high torque density, fault tolerance capability, redundancy and reliability [5]–[14].

The associate editor coordinating the review of this manuscript and approving it for publication was Kan Liu.

Three-phase PM motors with conventional or unconventional winding structures can be utilized as the building blocks for six, nine and more phases. If the number of phases is multiple of three, three-phase winding configurations with or without a phase shift could also be considered as the building block. While the design and modelling of the balanced multiple three-phase motors are investigated widely, there are very limited number of publications covering nine-phase PM motor design in literature with balanced winding structure [15]–[19]. In addition, a few studies have been reported in literature on six-phase and nine-phase PM motors with an unbalanced winding structure where it provides significant benefits such as extremely low cogging, ability to provide precise control at low speeds and low total harmonic distortion (THD) levels of back electro motor force (Back EMF) voltage [20]–[24] compared to balanced winding structure. There are several studies reported about nine-phase machine modelling and control techniques for the motors with conventional symmetric winding (SW) configuration [25]–[33].

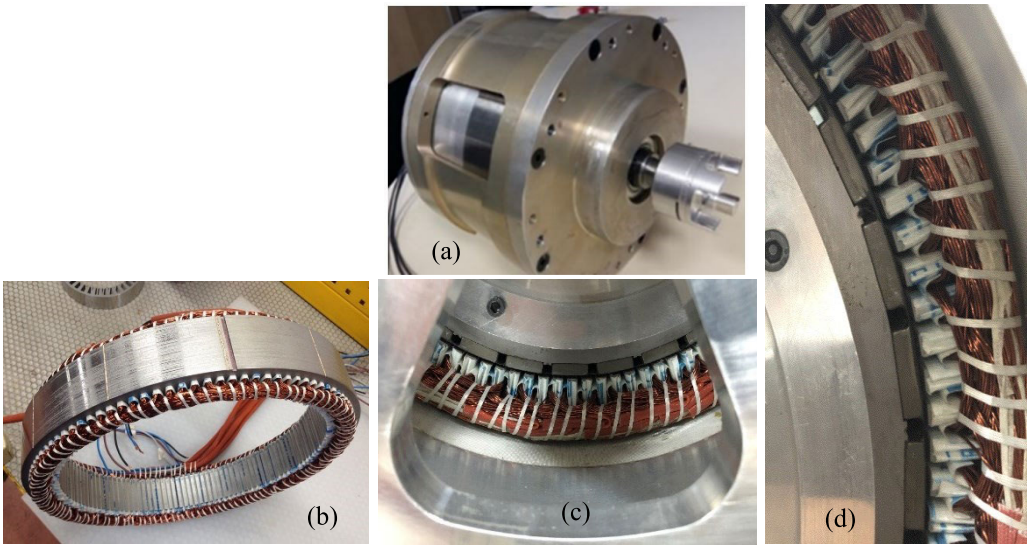

FIGURE 1. Previously designed 9-phase AW-SMPM Motor, (a) prototype motor, (b) stator housing, (c) airgap view and (d) rotor structure and magnet placement.

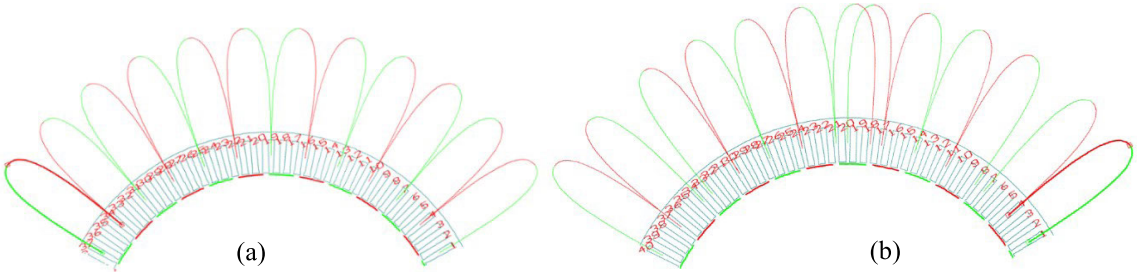

FIGURE 2. 3-phase winding distribution of the 9-phase PM motor (a) with 108 slots (q = 1 slot/pole/phase) and (b) 117 slots (q = 1.083 slot/pole/phase).

On the other hand, there is no modelling and verification study reported for the nine phase PM motors with asymmetric winding configuration.

In this paper, a full order mathematical model is introduced to a new 9-phase asymmetric winding surface mounted permanent magnet (AW-SMPM) motor. In order to obtain the electrical equations, the winding structure is first defined discretely and then using the Fourier series estimation a continuous form of the winding distribution is defined. In the proposed mathematical model, all the derivations are carried out based on the magneto motor force (MMF) functions and stator inductance matrix. In addition, the effects of asymmetric windings and unbalanced mutual inductance terms of the machine parameters have been examined in detail. Finally, experimental studies have been carried out for stator and *qd0* axes currents, inductances and torque output.

II. ANALYSIS OF THE NINE-PHASE AW-SMPM MOTOR

A. DESIGNED 9-PHASE MOTOR STRUCTURE

In this study, a 9-phase unconventional AW-SMPM motor has been examined and illustrated in the Fig.1. This motor has structural asymmetry in the stator and winding configuration, which results with the phase angles being different from 120 electrical degrees. Although the stator windings are placed asymmetrically, phase resistances have the same values. General specifications of the motor are given in the Table 1. Design of the 9-phase PM motor with odd number of slots and asymmetric winding configuration have been presented in earlier studies in order to achieve lower torque ripple without any stator or rotor skewing [21]. The main benefits of the AW-SMPM motor are the high torque quality and extremely low cogging component due to the odd fractional slot combination. Fig. 2 (a) shows the winding configurations of a conventional 9-phase motor with integer slot combinations (108 slot, 36 pole motor). Fig. 2 (b), on the other hand, shows the proposed asymmetric winding 9-phase PM motor with fractional slot combinations (117 slot, 36 pole motor). Detailed finite element analysis (FEA) simulations of the AW-SMPM motor with nine-phase 117-slot and 36-pole motor were completed and no-load flux density distribution of the motor is presented in the Fig. 3 (a-b). Furthermore, the obtained output torque and cogging torque variations from FEA are given in the Fig. 3 (c). FEA simulations were performed for 15A peak current value in order to be consistent with the experimental data. It is seen that 50.76 Nm average torque and approximately 0.02% cogging torque values are obtained. When the proposed 9-phase motor is compared with conventional 3-phase motor, it is observed

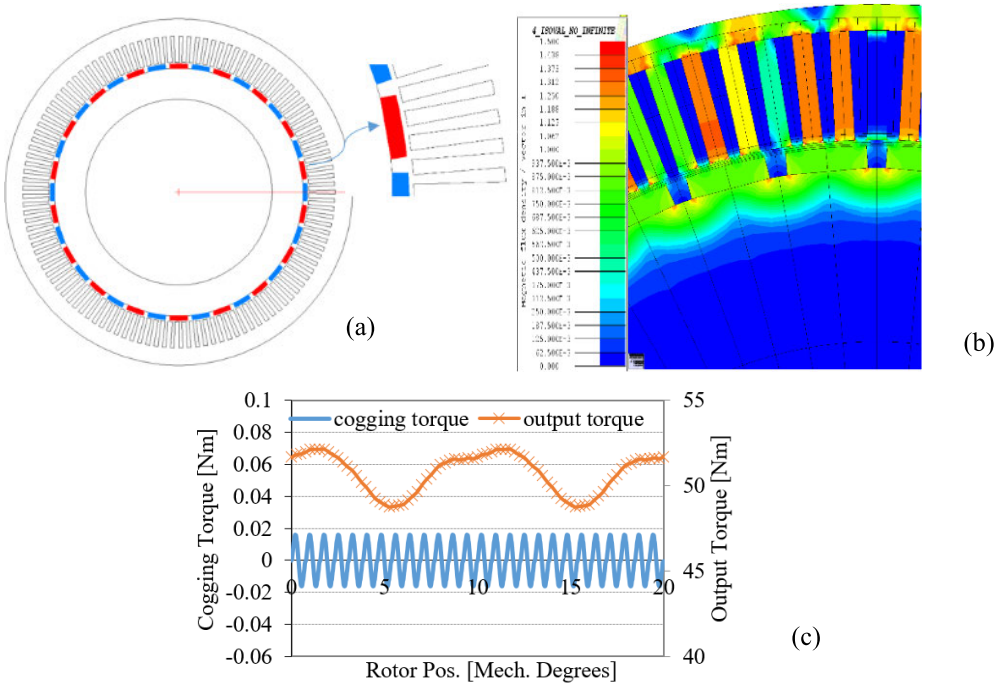

FIGURE 3. FEA process, (a) motor model, (b) no-load flux density distribution, (c) output torque and cogging torque variations.

TABLE 1. Motor parameters.

Symbol	Parameters	Value
T [Nm]	Rated torque	50.76
I [A]	Rated current	32
Qs	Slot numbers	117
m	Number of phases	9
L [mm]	Stator OD	370
P	Number of poles	36

that the torque-to-mass ratio (Nm/kg) as well as torque constant (Nm/Arms) becomes higher in 9-phase motors than its 3-phase counterparts. In addition, total losses are smaller in 9-phase motor resulting with higher efficiency. However, radial forces increase as the asymmetry is introduced at the winding configuration and additional torque ripple will be produced during operation. In order to highlight the advantages of the proposed 9-phase motor, FEA results comparing it to a conventional 9-phase design (with and without skewing) are summarized in Table 2. As seen from the table, although the rated torque value of the proposed motor is lower than a balanced 9-phase option, it offers less torque ripple percentage, cogging torque and THD level when compared to balanced 9-phase motor without skewing option.

B. ASYMMETRIC WINDING STRUCTURE AND PHASE ANGLES

In general, stator winding configurations of electrical machines can be categorized in four categories including integral slot winding, fractional slot concentrated winding with two options (where slot per pole per phase is fractional and lower than 1 and fractional and greater than 1) and unbalanced winding types. Nevertheless, in some cases a symmetric and balanced winding configuration cannot be achieved because of the slot-pole combinations. These kinds of electrical machines are referred to as unbalanced winding motors. The 9-phase winding configuration can be considered as three 3-phase winding sets, which are separated from each other by θ. Fig. 4 shows possible representations of the magnetic axes of stator winding of any 9-phase motor. In this figure, the winding vectors of 9-phase motor are labelled with ABCx, where x = 1,2,3 and denotes 3-phase winding set. Furthermore, α and β describes the electrical phase angles between the A1-B1 and A1-C1 windings, respectively. The other winding sets shifted by θ and 2θ electrical degrees with respect to A1-B1-C1. It is easily seen that several winding options can be designed by changing the angle between the winding sets. As a result, if α and β angles equal to 120 electrical degrees, motor become a balanced and symmetrical winding structure. In the designed 9-phase motor, α and β angles are designed as 116.04 and -116.74 electrical degrees, respectively and therefore an asymmetric winding configuration is created. Displacement of all winding sets along the stator circumference and the winding distribution of all nine phases are depicted in the Fig. 5. In order to determine the asymmetric phase angles (α and β), the individual coil electro motive force (EMF) vectors of each of the phases are used. In order to see the effect of the phase angles, a slightly worse case is examined in this paper.

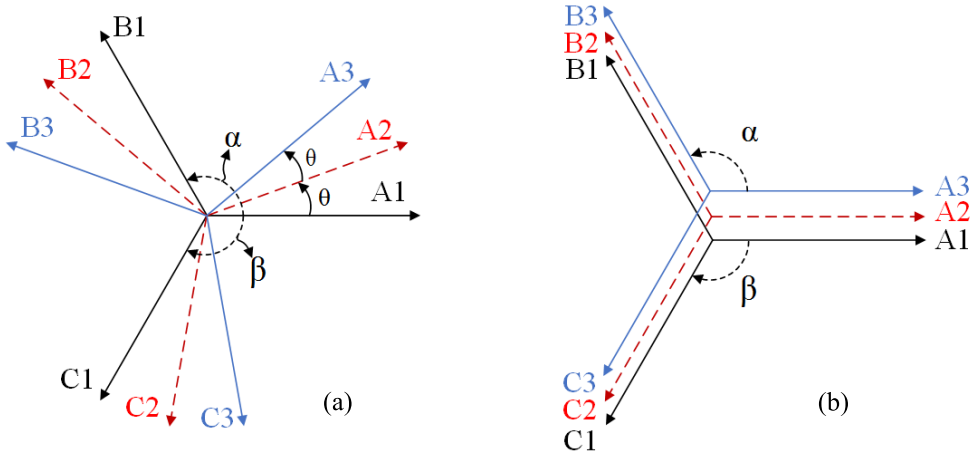

FIGURE 4. Vector of magnetic axes, (a) general representation for 9-phase motors, (b) proposed motor.

TABLE 2. Performance comparison between balanced 9-phase (integral slot) and unbalanced 9-phase (fractional slot) motor.

	108-Slot with 36-pole		117-Slot with 36-pole
	With Skew (θ_{skew}=3.33° mechanical)	Without Skew	Without Skew
DC Bus Voltage (V)	32		
Current per Phase (A)	19.03		15
Number of Turns	6		5
Peak to Peak Cogging Torque (Nm)	0.1	27.4	0.02
Rated Torque (Nm)	52.08	53.8	50.76
Rated Speed (rpm)	131	125	157
Torque Ripple Percentage	0.7	51.3	6.7
%THD for Line Back-EMF	0.25	2.2	1.34

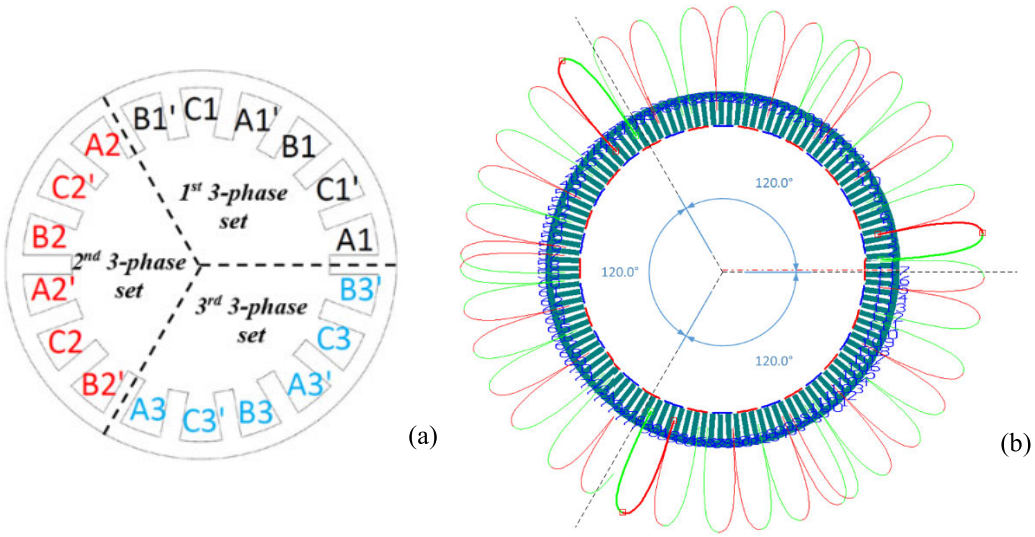

FIGURE 5. Motor design, (a) winding placement, (b) winding distribution of designed 9-phase asymmetric PM motor.

The winding function in discrete form is defined with respect to the positions of the stator slots, which is given for the first 3-phase set in the Fig. 6 (a). Then the continuous form of this discrete form of the winding function is defined via Fourier series approximation. According to the Fourier series approximation, the winding function of any phase of the machine is describe as:

$$w(\phi) = a_0 + \sum_{n=1}^{\infty} a_n \cos(n\phi) + b_n \sin(n\phi) \tag{1}$$

where a_n and b_n are the coefficients of the Fourier series, a_0 is the average value, n represents the harmonic numbers and

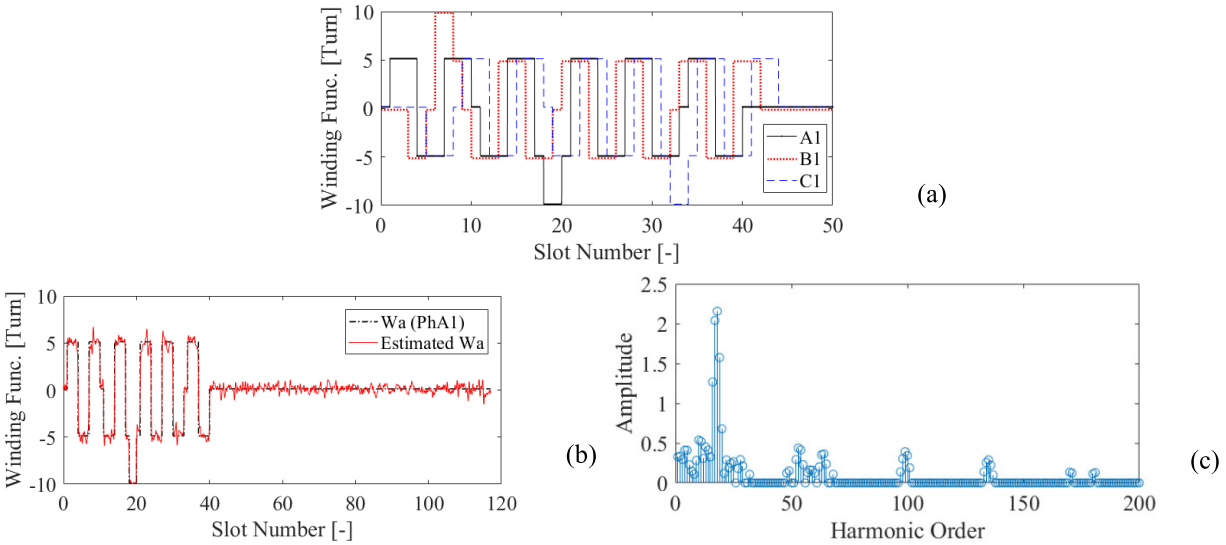

FIGURE 6. Winding distributions, (a) phase A1, B1 and C1, (b) calculated winding function of Phase A1, (c) harmonic components.

$\boldsymbol{\phi}$ denotes the position of stator circumference. Because of the winding functions are not symmetric and different from the conventional balanced windings, higher order harmonics are necessary to obtain accurate MMF distribution. Therefore, first 200 harmonic components are considered to obtain proper winding functions. The estimated winding function of phase A1 and its harmonic components are depicted in the Fig. 6 (b) and Fig. 6 (c) respectively.

C. INDUCTANCES AND FLUX LINKAGES

Since the proposed 9-phase motor is a surface mounted permanent magnet motor, the air gap function may be considered as a constant and expressed as:

$$g(\phi) = g_{ag} \tag{2}$$

The air gap flux density due to winding b, flux linkage and mutual inductance terms between phase-a and phase-b can be calculated with the following expressions. Where, if $a = b$ than the self-inductance of any phase can be obtained.

$$B_b(\phi) = \frac{\mu_0}{g(\phi)} w_b(\phi)\, i_b \tag{3}$$

$$\lambda_{ab} = \left(\mu_0\, rl \int_0^{2\pi} \frac{w_a(\phi)\, w_b(\phi)}{g(\phi)} d\phi\right) i_b \tag{4}$$

$$L_{ab} = \frac{\lambda_{ab}}{i_b} = \mu_0\, rl \int_0^{2\pi} \frac{w_a(\phi)\, w_b(\phi)}{g(\phi)} d\phi \tag{5}$$

where μ_0, r and l denote the vacuum permeability, radius of the stator inner frame and stack length, respectively. It has to be mentioned that the inductance expression given above consists of magnetizing inductance value.

Due to the fact that both the rated current of the motor is 32A and magnets are surface mounted, inductance values are not expected to be affected by saturation. In addition, since simulation studies and tests are performed below 32A rated current, saturation effects are not significant in the considered design.

III. MATHEMATICAL MODELLING AND SIMULATONS OF THE NINE-PHASE AW-SMPM MOTOR

The mathematical model helps provide physical understanding of the machine performance can be used in optimization process since it is faster compared to FEA and also it is useful from a control perspective. During the mathematical derivation process for the proposed PM motor, some limitations and assumptions are considered such as airgap distribution is considered perfectly sinusoidal, permeability of iron is considered infinite and the magnetic system is considered as linear. A mathematical model of the asymmetric 9-phase PM motor is developed based on per phase electrical equations, which can be written in the stationary stator reference frame as follows:

$$V_{abc-x} = r_s i_{abc-x} + \rho\lambda_{abc-x} \quad (x = 1, 2, 3) \tag{6}$$

where abc denotes the stator phases, x is number of the stator winding sets and ρ is time derivative.

In addition, V_{abc-x}, r_s, i_{abc-x}, λ_{abc-x} terms describe the phase voltages, stator winding resistance, phase currents and flux linkages, respectively. For a magnetically linear system, flux linkages of 9-phase permanent magnet motors in the stationary reference frame may be expressed as:

$$\lambda_{abc-x} = L_{abc-x} i_{abc-x} + \lambda_{m-abc-x} \quad (x = 1, 2, 3) \tag{7}$$

where L_{abc-x} and $\lambda_{m-abc-x}$ define the stator windings inductance matrix and magnet flux linkages, respectively. Since the 9-phase motor has structurally asymmetric windings, the angles between the stator magnetic axes are not equal to 120 electrical degrees and therefore, the transformation to an arbitrary reference frame is reconfigured with the values of

$\alpha = 116.04°$ and $\beta = -116.74°$ and given in (8):

$$A(\theta,\alpha,\beta) = \frac{2}{3}\begin{bmatrix} \cos(\theta) & \cos(\theta-\alpha) & \cos(\theta+\alpha) \\ \sin(\theta) & \sin(\theta-\beta) & \sin(\theta+\beta) \\ \frac{1}{2} & \frac{1}{2} & \frac{1}{2} \end{bmatrix}$$

$$T^*_{9\text{-phase}}(\theta,\alpha,\beta) = \begin{bmatrix} A & A & A \\ A & A & A \\ A & A & A \end{bmatrix} \quad (8)$$

Using the transformation matrix defined above, any variable in the stationary axes can be expressed in the rotating *qd0* axes via:

$$f_{qd0,123} = T^*_{9-phase}(\theta,\alpha,\beta) f_{abc,123} \quad (9)$$

where either voltage, current, flux linkage or the other machine terms can be represented by means of f. The flux linkages in *qd0* axes can be written with (10), as shown at the bottom of this page by using (9). In order to continue the analysis, we need to know the stator inductance matrix and magnet flux linkages. The stator inductance matrix (L_{abc-x}) of the 9-phase motor can be given in (24) where *abc-x* (x = *1, 2, 3*) denotes the winding sets and the inductance matrix consists of self and mutual inductance terms of the all three winding sets. In contrast to the machines with symmetrical winding structure, the mutual inductance values of each winding set of the proposed motor are obtained in different values, where $M_{ab-xy} \neq M_{ac-xy}$. On the other hand, flux linkages constituted by the permanent magnets can be described in matrix form in equation (11), as shown at the bottom of this page, where λ_m denotes the amplitude of the magnet flux linkages, α and β are phase angles (Fig. 4) and θ is the electrical rotor position. The second part on the right side of (10) refers to the magnet flux linkages in terms of *abc* axes variable and can be obtained in *qd0* by using the (9) as stated below:

$$\lambda_{qd0-x} = \lambda_m \begin{bmatrix} \delta_{q1} & \delta_{d1} & \delta_{01} & \delta_{q2} & \delta_{d2} & \delta_{02} & \delta_{q3} & \delta_{d3} & \delta_{03} \end{bmatrix}^T \quad (12)$$

where $\delta_{qd0-123}$ terms are the results of the matrix multiplication of (9) and (11) and are the function of electrical rotor position. Furthermore, the expanded version of $\delta_{qd0-123}$ terms are given in the appendix. Unlike the conventional motors, it can be seen from the above equation that the magnet flux has components on the q and *0* axes, albeit small. Because the all-magnetic axes of three winding sets are placed over each other and all *qd0* axes are mutually coupled, the following equation can be used for all elements of the inductance matrix.

$$T^*_{9-phase}(\theta,\alpha,\beta) f_{xy} T^*_{9-phase}(\theta,\alpha,\beta)^{-1} \quad (13)$$

In addition, how the (13) should be applied to the inductance matrix is given below:

$T(\theta)L_{11}T(\theta)^{-1}$	$T(\theta)M_{12}T(\theta)^{-1}$	$T(\theta)M_{13}T(\theta)^{-1}$
$T(\theta)M_{21}T(\theta)^{-1}$	$T(\theta)L_{22}T(\theta)^{-1}$	$T(\theta)M_{23}T(\theta)^{-1}$
$T(\theta)M_{31}T(\theta)^{-1}$	$T(\theta)M_{32}T(\theta)^{-1}$	$T(\theta)L_{33}T(\theta)^{-1}$

The obtained flux linkages matrix of the nine-phase motor is given in (25) where L_{qd0-x} and M_{qd0-xy} (x, y = *1, 2, 3*) are self and mutual synchronous inductance terms of 9-phase proposed motor. As seen from the *qd0* axes inductance matrix, there is no mutual inductance between qd_{xy} and 0_{xy} axes, although there occurs mutual inductance between the q_{xy} and d_{xy} axes. In addition, some mutually inductances (shown in red) in the same matrix have a negative effect on the output torque as it is calculated negatively. Furthermore, expanded equations of the flux linkage terms are given in (14-22) in the *qd0* rotating frame. Here, the flux linkages for the first 3-phase set are given in (14)–(16) as shown at bottom of this page. Similarly, flux linkage terms for the second 3-phase set are given in (17)–(19), as shown at bottom of the next page. Finally, flux linkages for the third 3-phase set are provided are given in (20)–(22), as shown at bottom of the next page, where λ_{qd0-x}, L_{qd0-x} and M_{qd0-x} describe the flux linkages terms, synchronous inductance and mutual inductance in the rotating *qd0* axes of each 3-phase winding sets, respectively. Here the flux linkage term M_{eff_AW} arises from the mutual inductances of the asymmetric windings and expanded versions also are given and dashed areas define the standard flux linkage terms.

If the transformation matrix $T^*(\theta,\alpha,\beta)$ and its inverse $T^*(\theta,\alpha,\beta)^{-1}$ are applied to the voltage equation that given in (6), voltage equations in terms of *qd0* axes variables can be obtained as stated below (26-28), as shown at the bottom of the next page. It is easily seen from the equations that all *qd0* axes voltages have coupled each other because of the flux linkage terms are given in (23)–(25), as shown at the bottom of the next page. Since the proposed 9-phase motor has three separate 3-phase winding sets, total electromagnetic

$$\lambda_{qd0-x} = T^*_{9-phase}(\theta,\alpha,\beta) L_{abc-x} T^*_{9-phase}(\theta,\alpha,\beta)^{-1} i_{qd0-x} + T^*_{9-phase}(\theta,\alpha,\beta)\lambda_{m-abc-x} \quad (10)$$

$$\lambda_{abc-x} = \lambda_m \begin{bmatrix} \sin(\theta) & \sin(\theta-\alpha) & \sin(\theta+\beta) & \sin(\theta) & \sin(\theta-\alpha) & \sin(\theta+\beta) & \sin(\theta) & \sin(\theta-\alpha) & \sin(\theta+\beta) \end{bmatrix}^T \quad (11)$$

$$\lambda_{q1} = \boxed{L_{q1}i_{q1}} + M_{eff\_AW\_q1} = L_{q1}i_{q1} + \left[M_{q1d1}i_{d1} + M_{q1q2}i_{q2} + M_{q1d2}i_{d2} + M_{q1q3}i_{q3} + M_{q1d3}i_{d3} + \lambda_m\delta_{q1}\right] \quad (14)$$

$$\lambda_{d1} = \boxed{L_{d1}i_{d1} + \lambda_m\delta_{d1}} + M_{eff\_AW\_d1} = L_{d1}i_{d1} + \lambda_m\delta_{d1} + \left[M_{d1q1}i_{q1} + M_{d1q2}i_{q2} + M_{d1d2}i_{d2} + M_{d1q3}i_{q3} + M_{d1d3}i_{d3}\right] \quad (15)$$

$$\lambda_{01} = \boxed{L_{01}i_{01}} + M_{eff\_AW\_01} = L_{01}i_{01} + [M_{0102}i_{02} + M_{0103}i_{03} + \lambda_m\delta_{01}] \quad (16)$$

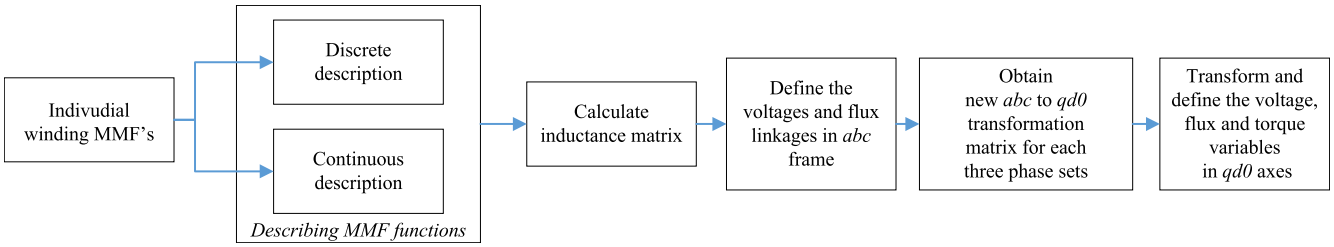

FIGURE 7. Overall flow-chart scheme of derivation process of the mathematical model.

output torque consists of sum of these three winding sets and can be described in (29) where j, λ_{qd} and i_{qd} define the number of the winding sets, flux linkages and currents, respectively. Additionally, the detailed torque output expressions can be given in (30-32) for each three winding sets. The left sides of the (30-32) are the conventional torque equations (dashed areas); the right sides, on other hand, are due to the asymmetry and coupling term. It is easily seen from the (30-32) that the output torque obtained from the each winding sets are interdependent with the inductances and qd axes currents of the other windings.

$$T_{e-total} = \sum_{j=1}^{3} \left(\frac{3}{2}\right)\left(\frac{P}{2}\right)\left(\lambda_{dj} i_{qj} - \lambda_{qj} i_{dj}\right) \tag{29}$$

$$\lambda_{q2} = \boxed{L_{q2} i_{q2}} + M_{eff\_AW\_q2} = L_{q2} i_{q2} + \left[M_{q2q1} i_{q1} + M_{q2d1} i_{d1} + M_{q2d2} i_{d2} + M_{q2q3} i_{q3} + M_{q2d3} i_{d3} + \lambda_m \delta_{q2}\right] \tag{17}$$

$$\lambda_{d2} = \boxed{L_{d2} i_{d2} + \lambda_m \delta_{d2}} + M_{eff\_AW\_d2} = L_{d2} i_{d2} + \lambda_m \delta_{d2} + \left[M_{d2q1} i_{q1} + M_{d2d1} i_{d1} + M_{d2q2} i_{q2} + M_{d2q3} i_{q3} + M_{d2d3} i_{d3}\right] \tag{18}$$

$$\lambda_{02} = \boxed{L_{02} i_{02}} + M_{eff\_AW\_02} = L_{02} i_{02} + \left[M_{0201} i_{01} + M_{0203} i_{03} + \lambda_m \delta_{02}\right] \tag{19}$$

$$\lambda_{q3} = \boxed{L_{q3} i_{q3}} + M_{eff\_AW\_q3} = L_{q3} i_{q3} + \left[M_{q3q1} i_{q1} + M_{q3d1} i_{d1} + M_{q3q2} i_{q2} + M_{q3d2} i_{d2} + M_{q3d3} i_{d3} + \lambda_m \delta_{q3}\right] \tag{20}$$

$$\lambda_{d3} = \boxed{L_{d3} i_{d3} + \lambda_m \delta_{d3}} + M_{eff\_AW\_d3} = L_{d3} i_{d3} + \lambda_m \delta_{d3} + \left[M_{d3q1} i_{q1} + M_{d3d1} i_{d1} + M_{d3q2} i_{q2} + M_{d3d2} i_{d2} + M_{d3q3} i_{q3}\right] \tag{21}$$

$$\lambda_{03} = \boxed{L_{03} i_{03}} + M_{eff\_AW\_03} = L_{03} i_{03} + \left[M_{0301} i_{01} + M_{0302} i_{02} + \lambda_m \delta_{03}\right] \tag{22}$$

$$V_{qd0-x} = T^*\left(\theta, \alpha, \beta\right) r_s T^*\left(\theta, \alpha, \beta\right)^{-1} i_{qd0-x} + T^*\left(\theta, \alpha, \beta\right) \rho \left[T^*\left(\theta, \alpha, \beta\right)^{-1} \lambda_{qd0-x}\right] \tag{23}$$

$$L_{abc-x} = \begin{bmatrix} L_{a1} & M_{a1b1} & M_{a1c1} & M_{a1a2} & M_{a1b2} & M_{a1c2} & M_{a1a3} & M_{a1b3} & M_{a1c3} \\ M_{b1a1} & L_{b1} & M_{b1c1} & M_{b1a2} & M_{b1b2} & M_{b1c2} & M_{b1a3} & M_{b1b3} & M_{b1c3} \\ M_{c1a1} & M_{c1b1} & L_{c1} & M_{c1a2} & M_{c1b2} & M_{c1c2} & M_{c1a3} & M_{c1b3} & M_{c1c3} \\ M_{a2a1} & M_{a2b1} & M_{a2c1} & L_{a2} & M_{a2b2} & M_{a2c2} & M_{a2a3} & M_{a2b3} & M_{a2c3} \\ M_{b2a1} & M_{b2b1} & M_{b2c1} & M_{b2a2} & L_{b2} & M_{b2c2} & M_{b2a3} & M_{b2b3} & M_{b2c3} \\ M_{c2a1} & M_{c2b1} & M_{c2c1} & M_{c2a2} & M_{c2b2} & L_{c2} & M_{c2a3} & M_{c2b3} & M_{c2c3} \\ M_{a3a1} & M_{a3b1} & M_{a3c1} & M_{a3a2} & M_{a3b2} & M_{a3c2} & L_{a3} & M_{a3b3} & M_{a3c3} \\ M_{b3a1} & M_{b3b1} & M_{b3c1} & M_{b3a2} & M_{b3b2} & M_{b3c2} & M_{b3a3} & L_{b3} & M_{b3c3} \\ M_{c3a1} & M_{c3b1} & M_{c3c1} & M_{c3a2} & M_{c3b2} & M_{c3c2} & M_{c3a3} & M_{c3b3} & L_{c3} \end{bmatrix} \tag{24}$$

$$\lambda_{qd0-xy} = \begin{bmatrix} L_{q1} & M_{q1d1} & 0 & M_{q1q2} & M_{q1q2} & 0 & M_{q1q3} & M_{q1d3} & 0 \\ M_{q1q1} & L_{d1} & 0 & M_{d1q2} & M_{d1d2} & 0 & M_{q1q3} & M_{d1d3} & 0 \\ 0 & 0 & L_{01} & 0 & 0 & M_{0102} & 0 & 0 & M_{0103} \\ M_{q2q1} & M_{q2d1} & 0 & L_{q2} & M_{q2d2} & 0 & M_{q2q3} & M_{q2d3} & 0 \\ M_{q2d1} & M_{d2d1} & 0 & M_{q2d2} & L_{d2} & 0 & M_{d2q3} & M_{d2d3} & 0 \\ 0 & 0 & M_{0201} & 0 & 0 & L_{02} & 0 & 0 & M_{0203} \\ M_{q3q1} & M_{q2d1} & 0 & M_{q3q2} & M_{q3d2} & 0 & L_{q3} & M_{q3d3} & 0 \\ M_{d3q1} & M_{d3d1} & 0 & M_{q2d2} & M_{d3d2} & 0 & M_{q2d3} & L_{d3} & 0 \\ 0 & 0 & M_{0301} & 0 & 0 & M_{0302} & 0 & 0 & L_{03} \end{bmatrix} \begin{bmatrix} i_{q1} \\ i_{d1} \\ i_{01} \\ i_{q2} \\ i_{d2} \\ i_{02} \\ i_{q3} \\ i_{d3} \\ i_{03} \end{bmatrix} + \lambda_m \begin{bmatrix} \delta_{q1} \\ \delta_{d1} \\ \delta_{01} \\ \delta_{q2} \\ \delta_{d2} \\ \delta_{02} \\ \delta_{q3} \\ \delta_{d3} \\ \delta_{03} \end{bmatrix} \tag{25}$$

$$V_{qx} = r_s i_{qx} + \omega \lambda_{dx} + \rho \lambda_{qx} \tag{26}$$

$$V_{dx} = r_s i_{dx} - \omega \lambda_{qx} + \rho \lambda_{dx} \tag{27}$$

$$V_{0x} = r_s i_{0x} + \rho \lambda_{0x} \tag{28}$$

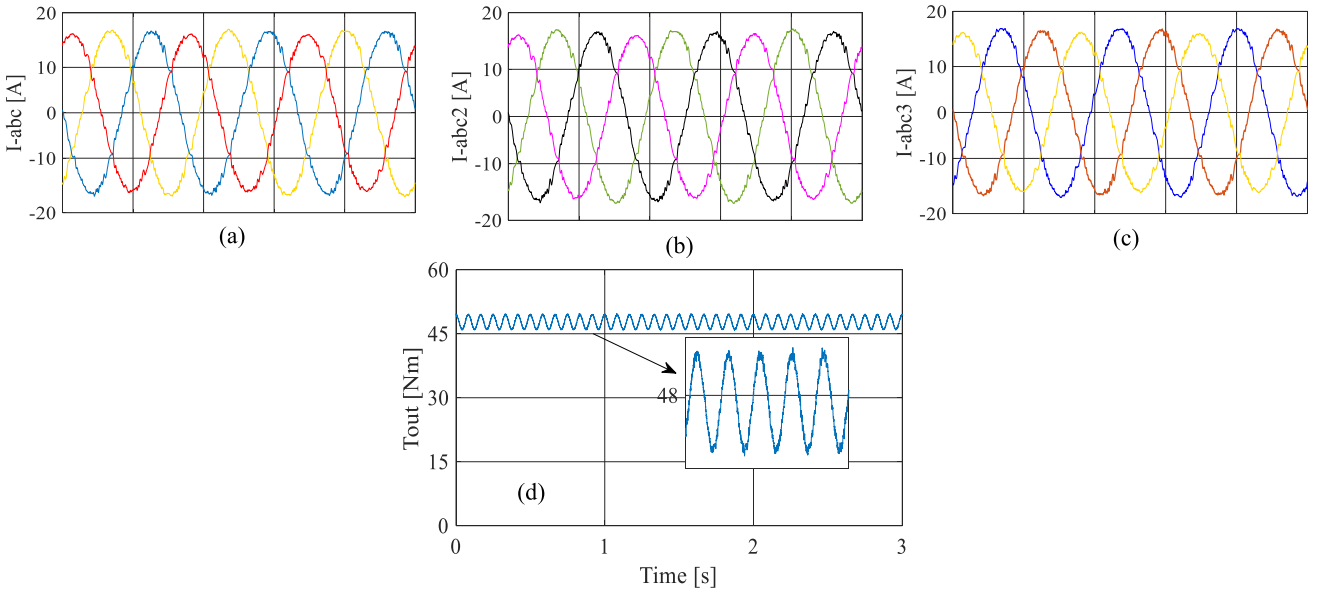

FIGURE 8. Simulation results; phase currents, (A) set1 (ABC1), (b) set2 (ABC2), (c) set3 (ABC3) and (d) output torque.

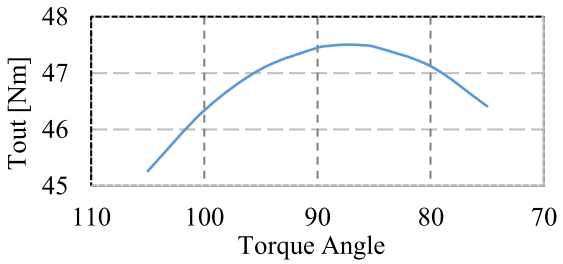

FIGURE 9. Simulation result of torque vs torque angle characteristic.

$$T_{e1} = \boxed{\left(L_{d1}i_{d1} + \lambda_m\delta_{d1}\right)i_{q1} - L_{q1}i_{q1}i_{d1}} + \left\{\left(M_{eff\_AW\_d1}\right)i_{q1} - \left(M_{eff\_AW\_q1}\right)i_{d1}\right\} \quad (30)$$

$$T_{e2} = \boxed{\left(L_{d2}i_{d2} + \lambda_m\delta_{d2}\right)i_{q2} - L_{q2}i_{q2}i_{d2}} + \left\{\left(M_{eff\_AW\_d2}\right)i_{q2} - \left(M_{eff\_AW\_q2}\right)i_{d2}\right\} \quad (31)$$

$$T_{e3} = \boxed{\left(L_{d3}i_{d3} + \lambda_m\delta_{d3}\right)i_{q3} - L_{q3}i_{q3}i_{d3}} + \left\{\left(M_{eff\_AW\_d3}\right)i_{q3} - \left(M_{eff\_AW\_q3}\right)i_{d3}\right\} \quad (32)$$

where $M_{eff\_AW\_qd}$ terms arise from the asymmetric winding structure, which do not exist in the conventional symmetric winding machines and are defined in (14-22).

Furthermore, overall flow chart of derivation process of the mathematical modelling is summarized in the Fig. 7. It has to be pointed out that development process of the mathematical modelling is suitable for all of the 3, 6 or 12 etc. phase motors regardless of the SPM or IPM rotor structures.

The Matlab-Simulink model of the proposed 9-phase AW-SMPM motor is generated to see the accuracy of the mathematical model obtained in the previous section. In the simulation study, 15A current value is given as a reference signal for the each three-phase winding sets, and the results are shown in the Fig. 8 (a-c). Although all the peak values of

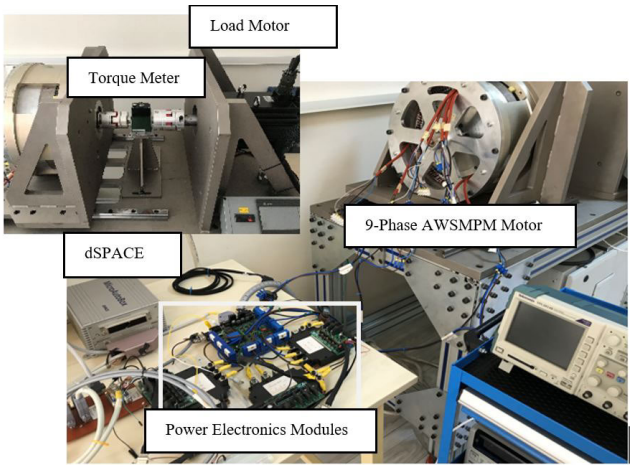

FIGURE 10. Experimental test system of the proposed 9-phase motor.

stator currents are about 15A, there occur small differences between the peak values of phase currents due to asymmetric winding and unbalanced mutual inductances. Moreover, the obtained torque output is also given in the Fig. 8 (d). FEA show that 50.76Nm average torque is obtained with 6.7% torque ripple while 48.73Nm average torque is obtained with 6.28% torque ripple using the motor model presented.

There is roughly 4% error between the FEA and the model presented. Since the proposed 9-phase motor has asymmetric stator windings and has unbalanced self and mutual inductances, the maximum torque value has been obtained at an angle different from 90° electrical angle. Simulation has been performed based on the electrical equations given in previous section for the rated values. Fig. 9 shows the variation of output torque value in terms of three winding sets and total torque. For the proposed motor, maximum torque is obtained at nearly 88.5° torque angle for all three phase winding sets. It is clearly seen that the positive d axis current value

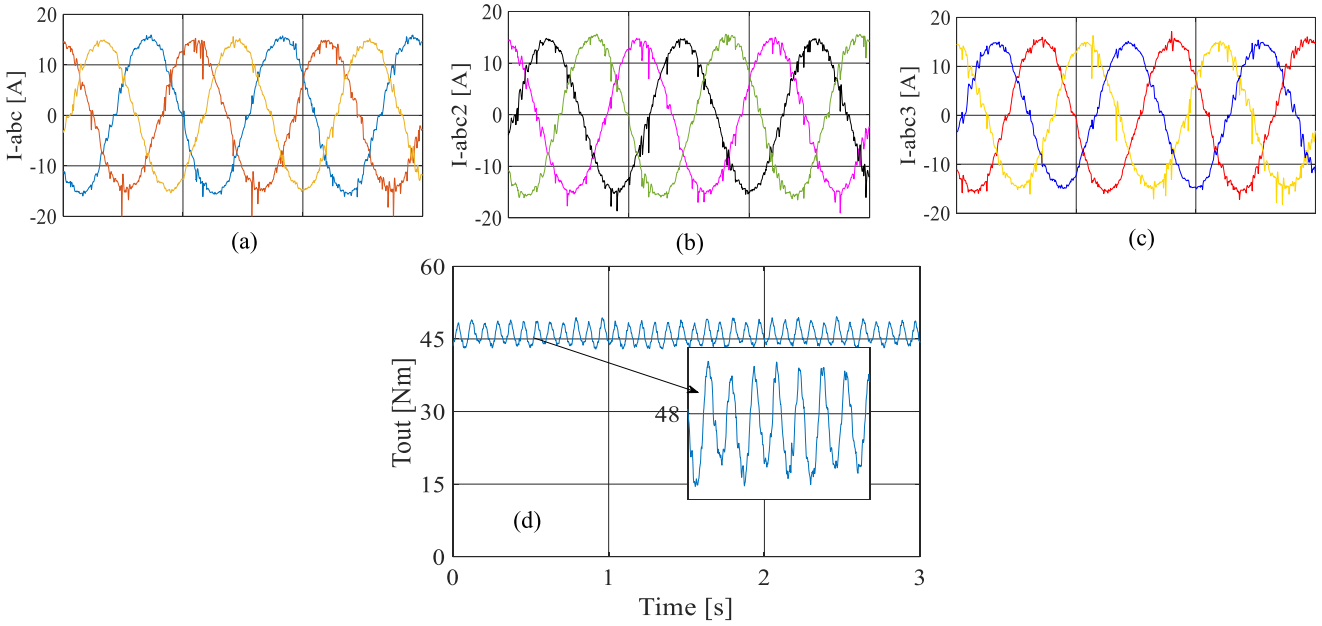

FIGURE 11. Experimental results; phase currents, (a) set1 (ABC1), (b) set2 (ABC2), (c) set3 (ABC3), (d) total output torque.

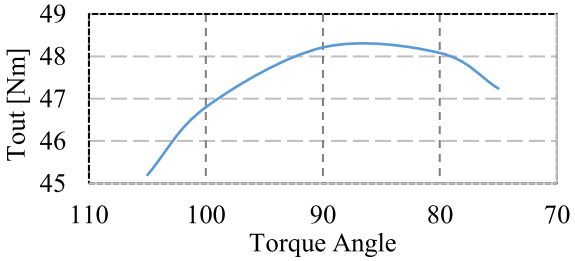

FIGURE 12. Test result of torque vs torque angle characteristic.

TABLE 3. Comparison of the obtained torque outputs.

	Average Torque (@15A)	%Torque Ripple	% Error on Avg. Torque
2D-FEA	50.76Nm	6.7%	---
Math. Model	48.73Nm	6.28%	4%
Experimental	48.17Nm	8.57%	5.1%

increases the total torque output since it reduces the effect of unbalanced negative inductances.

IV. EXPERIMENTAL RESULTS AND COMPARISON

The prototype motor is tested and the results are presented to see the accuracy of FEA and developed mathematical model. The experimental setup consists of dSPACE MicroAutobox II, three IGBT (insulated gate bipolar transistor) power electronic modules, proposed 9-phase motor, load motor and torque meter are illustrated in the Fig. 10. During the experimental studies, 15A peak currents are given as a reference signal to the all-winding sets because of the output torque limitation of the load motor.

The test results are illustrated in the Fig. 11. As seen from the figure, stator currents are obtained as desired with some harmonic components and different peak values as in the simulation. Moreover, output torque data has a 48.17 Nm

TABLE 4. Comparison of the average torque outputs at the difference current values.

Peak current per 3phase set	Math. Model Avg. Torque	Experimental Avg. Torque	% Error on Avg. Torque
@5A	15.31 Nm	15.01 Nm	1.99%
@10A	31.83 Nm	31.44 Nm	1.44%
@15A	48.73 Nm	48.17 Nm	1.16%
@20A	64.07 Nm	63.31 Nm	1.2%

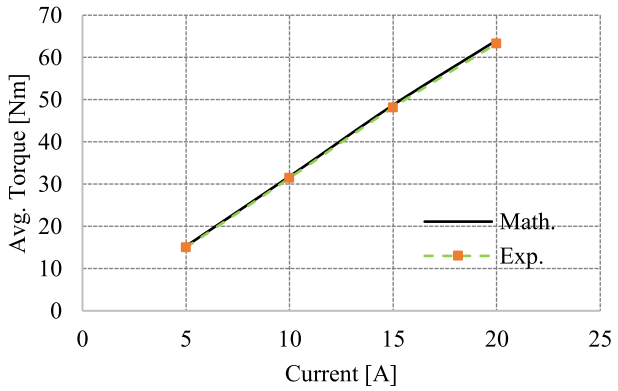

FIGURE 13. Comparison of average torque outputs.

average value with 8.57% torque ripple although 2D-FEA provides 6.7%, mathematical model provides 6.28% ripple the discrepancy is arising from the test setup alignment. It has obviously been noticed that there is a good agreement between FEA, simulation and experimental studies.

On the other hand, maximum torque for all three phase winding sets (Fig.12) is obtained at a torque angle of 87° which is very close with mathematical model (88.5°). Comparison of the obtained torque data between FEA, simulation and experimental study is also presented in Table 3.

In order to show the accuracy of the mathematical model, different values of currents are given as a reference signal to the controller and the obtained results are summarized in Table 4 and Fig. 13. It can be concluded that there is a good agreement between mathematical modelling and test results and the developed model provides results with less than 2% error compared to test results.

V. CONCLUSION

In conclusion, this paper presents a full order mathematical description, modelling, FEA simulations and experimental verification for a previously designed unconventional 9-phase AW-SMPM synchronous motor. Detailed mathematical derivations are obtained in terms of flux linkages, voltages, inductances and torque equations are presented. Dynamic machine equations of the proposed 9-phase AW-SMPM motor are attained based on the winding functions of all phases and observed separately for the triple 3-phase winding sets. It is perceived that asymmetric and unbalanced stator currents occur in this type of winding configurations and cause oscillations on dq axes currents and torque output. The fact that some of the mutual inductance values are negative lessens the output torque although it is fairly small in the proposed 9-phase motor. Furthermore, the mathematical findings are confirmed with both FEA and experimental results. Finally, it can be concluded that the proposed 9-phase motor can be controlled by a control strategy that will eliminate the drawbacks of the asymmetric windings.

APPENDIX

In this section, the obtained results in terms of expanded versions of the magnet flux linkage terms are presented. In the proposed motor, coefficients of the magnet flux linkage changes sinusoidal on the contrary of conventional symmetric winding motors. This indicates that the magnet flux has components both in q and 0 axes in addition to the d axis.

$$\delta_{q-123} = \frac{\cos\left(2\theta + 37.92^\circ\right)}{3} + \frac{\sin\left(2\theta\right)}{3} - \frac{\sin\left(2\theta + \beta + \alpha - 180^\circ\right)}{3}$$

$$\delta_{d-123} = \frac{2\cos\left(\theta + \beta - 90^\circ\right)^2}{3} + \frac{2\sin\left(\theta\right)^2}{3} + \frac{2\sin\left(\theta - \alpha + 180^\circ\right)^2}{3}$$

$$\delta_{0-123} = \frac{\cos\left(\theta + \beta - 90^\circ\right)}{3} + \frac{\sin\left(\theta\right)}{3} + \frac{\sin\left(\theta - \alpha + 180^\circ\right)}{3}$$

where α, β are the angles between the stator magnetic axes (Fig. 4) and θ denotes rotor position

REFERENCES

[1] T. Sebastian, G. Slemon, and M. Rahman, "Modelling of permanent magnet synchronous motors," *IEEE Trans. Magn.*, vol. 22, no. 5, pp. 1069–1071, Sep. 1986.

[2] M. A. Rahman and T. A. Little, "Dynamic performance analysis of permanent magnet synchronous motors," *IEEE Power Eng. Rev.*, vol. PER–4, no. 6, p. 40, Jun. 1984.

[3] A. Takbash, M. Ibrahim, and P. Pillay, "Design optimization of a spoke-type variable flux motor using AlNiCo for electrified transportation," *IEEE Trans. Transport. Electrific.*, vol. 4, no. 2, pp. 536–547, Jun. 2018.

[4] T. M. Jahns, G. B. Kliman, and T. W. Neumann, "Interior permanent-magnet synchronous motors for adjustable-speed drives," *IEEE Trans. Ind. Appl.*, vol. IA–22, no. 4, pp. 738–747, Jul. 1986.

[5] F. Yu, W. Zhang, Y. Shen, and J. Mao, "A nine-phase permanent magnet electric-drive-reconstructed onboard charger for electric vehicle," *IEEE Trans. Energy Convers.*, vol. 33, no. 4, pp. 2091–2101, Dec. 2018.

[6] Y. Shi and J. Wang, "Continuous demagnetisation assessment for triple redundant nine-phase fault-tolerant permanent magnet machine," *J. Eng.*, vol. 2019, no. 17, pp. 4359–4363, Jun. 2019.

[7] A. Mohammadpour, S. Mishra, and L. Parsa, "Fault-tolerant operation of multiphase permanent-magnet machines using iterative learning control," *IEEE J. Emerg. Sel. Topics Power Electron.*, vol. 2, no. 2, pp. 201–211, Jun. 2014.

[8] M. Ruba and D. Fodorean, "Analysis of fault-tolerant multiphase power converter for a nine-phase permanent magnet synchronous machine," *IEEE Trans. Ind. Appl.*, vol. 48, no. 6, pp. 2092–2101, Nov. 2012.

[9] B. Wang, J. Wang, A. Griffo, and B. Sen, "Experimental assessments of a triple redundant nine-phase fault-tolerant PMA SynRM drive," *IEEE Trans. Ind. Electron.*, vol. 66, no. 1, pp. 772–783, Jan. 2019.

[10] A. G. Sarigiannidis, M. E. Beniakar, P. E. Kakosimos, A. G. Kladas, L. Papini, and C. Gerada, "Fault tolerant design of fractional slot winding permanent magnet aerospace actuator," *IEEE Trans. Transport. Electrific.*, vol. 2, no. 3, pp. 380–390, Sep. 2016.

[11] E. Jung, H. Yoo, S.-K. Sul, H.-S. Choi, and Y.-Y. Choi, "A nine-phase permanent-magnet motor drive system for an ultrahigh-speed elevator," *IEEE Trans. Ind. Appl.*, vol. 48, no. 3, pp. 987–995, May 2012.

[12] E. Levi, F. Barrero, and M. J. Duran, "Multiphase machines and drives–revisited," *IEEE Trans. Ind. Electron.*, vol. 63, no. 1, pp. 429–432, Jan. 2016.

[13] J. Huang, M. Kang, J. Q. Yang, H.-B. Jiang, and D. Liu, "Multiphase machine theory and its applications," in *Proc. Int. Conf. Electr. Mach. Syst.*, Wuhan, China, Oct. 2008, pp. 1–7.

[14] M. M. Wogari and O. Ojo, "Nine-phase interior permanent magnet motor for electric vehicle drive," in *Proc. IEEE Power Energy Soc. Gen. Meeting*, San Diego, CA, USA, Jul. 2011, pp. 1–8.

[15] E. Levi, "Multiphase electric machines for variable-speed applications," *IEEE Trans. Ind. Electron.*, vol. 55, no. 5, pp. 1893–1909, May 2008.

[16] A. S. Abdel-Khalik, S. Gadoue, and S. Ahmed, "A nine-phase six-terminal fractional-slot-winding for interior permanent-magnet machines with low space harmonics," in *Proc. 13th Int. Conf. Electr. Mach. (ICEM)*, Alexandroupoli, Greece, Sep. 2018, pp. 499–505.

[17] S. Brisset, D. Vizireanu, and P. Brochet, "Design and optimization of a nine-phase axial-flux PM synchronous generator with concentrated winding for direct-drive wind turbine," *IEEE Trans. Ind. Appl.*, vol. 44, no. 3, pp. 707–715, May/Jun. 2008.

[18] M. Cheng, J. Wang, S. Zhu, and W. Wang, "Loss calculation and thermal analysis for nine-phase flux switching permanent magnet machine," *IEEE Trans. Energy Convers.*, vol. 33, no. 4, pp. 2133–2142, Dec. 2018.

[19] X. Chen, J. Wang, V. I. Patel, and P. Lazari, "A nine-phase 18-slot 14-pole interior permanent magnet machine with low space harmonics for electric vehicle applications," *IEEE Trans. Energy Convers.*, vol. 31, no. 3, pp. 860–871, Sep. 2016.

[20] M. Onsal, Y. Demir, and M. Aydin, "A new nine-phase permanent magnet synchronous motor with consequent pole rotor for high-power traction applications," *IEEE Trans. Magn.*, vol. 53, no. 11, pp. 1–6, Nov. 2017.

[21] Y. Demir, E. Yolacan, A. M. EL-Refaie, and M. Aydin, "Investigation of different winding configurations and displacements of a nine-phase permanent-magnet-synchronous motor with unbalanced AC winding structure," *IEEE Trans. Ind. Appl.*, vol. 55, no. 4, pp. 3660–3670, Jul./Aug. 2019.

[22] E. Yolacan, Y. Demir, and M. Aydin, "Design, FEA and dynamic simulation of a new Unconventional9-phase PMSM with asymmetric winding," in *Proc. 13th Int. Conf. Electr. Mach. (ICEM)*, Alexandroupoli, Greece, Sep. 2018, pp. 2123–2129.

[23] Y. Demir and M. Aydin, "A novel dual three-phase permanent magnet synchronous motor with asymmetric stator winding," *IEEE Trans. Magn.*, vol. 52, no. 7, pp. 1–5, Jul. 2016.

[24] Y. Demir and M. Aydin, "A novel asymmetric and unconventional stator winding configuration and placement for a dual three-phase surface PM motor," *IEEE Trans. Magn.*, vol. 53, no. 11, pp. 1–5, Nov. 2017.
[25] M. Ramezani and O. Ojo, "The modeling and position-sensorless estimation technique for a nine-phase interior permanent-magnet machine using high-frequency injections," *IEEE Trans. Ind. Appl.*, vol. 52, no. 2, pp. 1555–1565, Mar./Apr. 2016.
[26] M. Cheng, F. Yu, K. T. Chau, and W. Hua, "Dynamic performance evaluation of a nine-phase flux-switching permanent-magnet motor drive with model predictive control," *IEEE Trans. Ind. Electron.*, vol. 63, no. 7, pp. 4539–4549, Jul. 2016.
[27] F. Scuiller, E. Semail, and J.-F. Charpentier, "General modeling of the windings for multi-phase ac machines: Application for the analytical estimation of the mutual stator inductances for smooth air gap machines," *Eur. Phys. J. Appl. Phys.*, vol. 50, no. 3, p. 31102, 2010.
[28] A. Gautam, S. Karugaba, and J. Ojo, "Modeling of nine-phase interior permanent magnet machines (IPM) including harmonic effects," in *Proc. IEEE Int. Electr. Mach. Drives Conf. (IEMDC)*, May 2011, pp. 681–686.
[29] O. Ojo, M. Ramezani, and A. Gautam, "Sensor-less vector control of the nine-phase concentrated wound interior permanent magnet motor drive using a unique third sequence high frequency injection into the stator windings," in *Proc. IEEE Energy Convers. Congr. Expo. (ECCE)*, Sep. 2015, pp. 853–859.
[30] A. Tessarolo, S. Mohamadian, and M. Bortolozzi, "A new method for determining the leakage inductances of a nine-phase synchronous machine from no-load and short-circuit tests," *IEEE Trans. Energy Convers.*, vol. 30, no. 4, pp. 1515–1527, Dec. 2015.
[31] A. Rockhill and T. A. Lipo, "A simplified model of a nine-phase synchronous machine using vector space decomposition," *Electr. Power Compon. Syst.*, vol. 38, no. 4, pp. 477–489, Jan. 2010.
[32] M. Ramezani and O. Ojo, "Coupled and simplified models of the symmetrical and asymmetrical triple-star nine-phase interior permanent magnet machines," in *Proc. IEEE Energy Convers. Congr. Expo. (ECCE)*, Milwaukee, WI, USA, Sep. 2016, pp. 1–8.
[33] F. Yu, M. Cheng, and K. T. Chau, "Controllability and performance of a nine-phase FSPM motor under severe five open-phase fault conditions," *IEEE Trans. Energy Convers.*, vol. 31, no. 1, pp. 323–332, Mar. 2016.

ERSIN YOLACAN (Member, IEEE) received the B.S., M.S., and Ph.D. degrees in mechatronics engineering from Kocaeli University, Kocaeli, Turkey, in 2009, 2012, and 2020, respectively. He is currently a Research Assistant with Kocaeli University. His research interests include electric motor drives, multiphase pm machines, modeling, power electronics, simulation, and real-time control of electrical machines.

MUSTAFA K. GUVEN (Senior Member, IEEE) received the B.Sc. degree in electrical engineering from Istanbul Technical University, Istanbul, Turkey, in 1993, specializing on microprocessor-based industrial system, and the M.S. and Ph.D. degrees in electrical engineering from The Ohio State University, Columbus, OH, USA, in 1997 and 2001, respectively, specializing in control system theory and in power electronics, electric machines, and drives. His current research interests include advance control theory, digital signal processors, and their applications in controlling motion systems, electric machine design and control, and power electronics. He also holds six patents in the areas of electric machine and their control. He has been a Senior Member of the Industry Application Society, since 2001.

METIN AYDIN (Member, IEEE) received the M.S. and Ph.D. degrees from the University of Wisconsin–Madison, in 1997 and 2004, respectively, all in electrical engineering. He worked with Wisconsin Electrical Machines and Power Electronics Consortium in Madison, for eight years, and Caterpillar Inc., Research and Development in Peoria, for more than two years. He is currently working as a Faculty Member with the Department of Mechatronics Engineering, Kocaeli University, Turkey. His research interests include conventional and un-conventional electrical machine design and control.

AYMAN M. EL-REFAIE (Fellow, IEEE) received the M.S. and Ph.D. degrees in electrical engineering from the University of Wisconsin–Madison, in 2002 and 2005, respectively. Since 2005, he has been with the Electrical Machines and Drives Laboratory, General Electric Global Research Center, Albany, NY, USA, as a Principal Engineer and a Project Leader. Since January 2017, he has also been the Thomas and Suzanne Werner Endowed Chair of secure and sustainable energy with Marquette University. He has appeared as an author or coauthor in 40 journals, and has 65 conference publications. He holds 38 issued U.S. patents, and 22 U.S. patent applications. His research interests include electrical machines and drives.